Science. Author manuscript; available in PMC 2016 September 16.

Published in final edited form as:
Science. 2010 August 13; 329(5993): 805–810. doi:10.1126/science.1191542.

Peripheral Protein Quality Control Removes Unfolded CFTR from the Plasma Membrane

Tsukasa Okiyoneda[1], **Hervé Barrière**[1], **Miklós Bagdány**[1], **Wael M. Rabeh**[1], **Kai Du**[1], **Jörg Höhfeld**[2], **Jason C. Young**[3], and **Gergely L. Lukacs**[1,*]

[1]Department of Physiology and Groupe de Recherche Axé sur la Structure des Protéine (GRASP), McGill University, Montreal, Quebec H3G 1Y6, Canada

[2]Cell Biology Institute, University Bonn, D-53121 Bonn, Germany

[3]Department of Biochemistry and Groupe de Recherche Axé sur la Structure des Protéine (GRASP), McGill University, Montreal, Quebec H3G 1Y6, Canada

Abstract

Therapeutic efforts to restore biosynthetic processing of the cystic fibrosis transmembrane conductance regulator lacking the F508 residue (ΔF508CFTR) are hampered by ubiquitin-dependent lysosomal degradation of nonnative, rescued ΔF508CFTR from the plasma membrane. Here, functional small interfering RNA screens revealed the contribution of chaperones, cochaperones, and ubiquitin-conjugating and -ligating enzymes to the elimination of unfolded CFTR from the cell surface, as part of a peripheral protein quality-control system. Ubiquitination of nonnative CFTR was required for efficient internalization and lysosomal degradation. This peripheral protein quality-control mechanism probably participates in the preservation of cellular homeostasis by degrading damaged plasma membrane proteins that have escaped from the endoplasmic reticulum quality control or are generated by environmental stresses in situ.

Aberrant polypeptides are generated as a consequence of errors in transcription, translation, and folding, as well as genetic mutations or environmental stress (1–3). To preserve proteostasis, quality-control (QC) mechanisms have evolved to facilitate folding and elimination of terminally misfolded polypeptides (3, 4). At the endoplasmic reticulum (ER), non-native membrane proteins are ubiquitinated and retrotranslocated into the cytoplasm to be destroyed by the ubiquitin (Ub) proteasome system (UPS), as part of ER-associated degradation (ERAD). By contrast, nonnative membrane proteins that have escaped the ER or are generated in post-ER compartments are preferentially eliminated by lysosomal degradation (5–7). The molecular machinery of the peripheral QC responsible for

*To whom correspondence should be addressed. gergely.lukacs@mcgill.ca.

Supporting Online Material
www.sciencemag.org/cgi/content/full/science.1191542/DC1
Materials and Methods
Figs. S1 to S10
Tables S1 to S4
References

recognition and degradation of nonnative proteins at plasma membrane (PM) remains unknown (1, 8–10).

Deletion of the F508 residue (ΔF508), the most prevalent mutation in the cystic fibrosis transmembrane conductance regulator (CFTR), causes a temperature-sensitive folding defect and ERAD of immature, core-glycosylated ΔF508CFTR by the concerted action of chaperones, cochaperones, and E2 Ub-conjugating and E3 Ub-ligating enzymes [carboxyl-terminus heat shock cognate 70 (Hsc70)–interacting protein (CHIP), glycoprotein gp78, and Rma1] (11–14). Although inhibition of individual E3-ligases failed to restore biosynthetic processing, low temperature (26°C) and small-molecule correctors alone, or in combination with the ablation of E3 ligases, fosters PM accumulation of functional, complex-glycosylated ΔF508CFTR (15–18). The rescued (r)ΔF508CFTR, however, is metabolically unstable and is rapidly eliminated at 37°C, which hampers therapeutic efforts to restore the PM chloride conductance (5, 18). Mutant CFTR instability was attributed to unfolding and subsequent ubiquitination, internalization, and lysosomal degradation (5, 6).

rΔF508CFTR as a probe of peripheral QC

To identify the rΔF508CFTR ubiquitination mechanism, we generated CFTR-3HA–expressing HeLa and IB3 (bronchial respiratory epithelia) cell lines amenable to small interfering RNA (siRNA) functional screens (19). The extracellular hemagglutinin tag (3HA-tag) enabled selective detection of CFTR (5). The wild-type (wt) protein was largely complex-glycosylated and localized to PM, whereas ΔF508CFTR was expressed as a core-glycosylated form and retained in the ER at 37°C (fig. S1, A to C). Rescuing the folding defect at 26°C (15) partially restored biosynthetic processing and expression of complex-glycosylated ΔF508CFTR at post-Golgi compartments and PM (fig. S1, A to C). Then, rΔF508CFTR was eliminated by accelerated internalization and attenuated recycling at 37°C (Fig. 1, A and B, and fig. S1, D to F) as expected (5).

A temperature-sensitive conformational defect of rΔF508CFTR was demonstrated by its protease susceptibility in isolated microsomes from BHK cells (20). Newly synthesized core-glycosylated channels were cleared from ER by cycloheximide (CHX) chase (~10 hours) at 26°C to avoid unfolding of complex-glycosylated rΔF508CFTR (fig. S1G). The trypsin susceptibility of rΔF508CFTR was increased 5- to 10-fold after unfolding at 37°C (2.5 hours) before microsome isolation (Fig. 1C). Mature wt CFTR and immature ΔF508CFTR had substantially lower and higher trypsin susceptibility, respectively, than rΔF508CFTR (Fig. 1C), as expected (21).

Denaturing immunoprecipitation (d-IP) and anti-Ub immunoblotting revealed a twofold increased ubiquitination of complex-glycosylated rΔF508CFTR after thermal unfolding (Fig. 1D). In the absence of unfolding, rΔF508CFTR PM stability, internalization, endocytic recycling, and ubiquitination level approached the wt phenotype (Fig. 1, A to D). In contrast, temperature dependence of the CD4Tl-Ub chimera PM instability (22) (fig. S1H), ubiquitination of cellular proteins, and Ub-ligase activity of CHIP (see below) were negligible (fig. S2, A to C). These observations are in line with the notion that conformational destabilization accounts for augmented rΔF508CFTR ubiquitination and fast

PM turnover at 37°C. Indeed, dramatically augmented trypsin susceptibility of ΔF508CFTR paralleled its ~100-fold increased ubiquitination at ER as compared with wt CFTR (Fig. 1, C and D). Thus, CFTR's propensity for ubiquitination is enhanced with its conformational destabilization, not only at ER, but also in post-Golgi compartments, and rΔF508CFTR is a suitable model to investigate the conformation-based QC at PM.

Supporting the function of ubiquitination in CFTR lysosomal degradation, ablation or knockdown (KD) of Hrs, STAM, or TSG101 Ub-binding constituents of the endosomal sorting complex required for transport (ESCRT) using individual or SMARTpool siRNA; (5, 6) metabolically stabilized rΔF508CFTR in HeLa cells (Fig. 1, E and F and fig. S3, A to C). This could be attributed to impeded lysosomal delivery, monitored by lumenal acidification extent, and rate of endocytic vesicles containing fluorescein isothiocyanate–labeled rΔF508CFTR (fig. S3, D to F). Lysosomal targeting of Lamp1 from PM was not influenced by the ESCRT KD (fig. S3E).

CHIP-dependent ubiquitination removes unfolded CFTR from PM

To identify the ubiquitination machinery of rΔF508CFTR, 33 E3 ligases involved in down-regulation of PM receptors (8, 10, 23) and CFTR ERAD (12, 13, 24) were depleted (knocked down) using SMARTpool siRNA, followed by determination of rΔF508CFTR PM stability in HeLa cells. CHIP, gp78, or Hrd1 depletion inhibited the rΔF508CFTR disposal by ~50% (Fig. 2A). Because only the CHIP effect could be confirmed in IB3 cells (Fig. 2B), subsequent experiments focused on CHIP. Individual CHIP siRNA also impeded complex-glycosylated and PM rΔF508CFTR degradation (Fig. 2C and fig. S4, A and B).

Internalization of unfolded rΔF508CFTR was diminished by ~80% upon CHIP KD without affecting transferrin receptor (TfR) and CD4Tcc-Ub (AllRΔG) chimera uptake, signaled by tyrosine-and tetrameric Ub-based endocytic motifs, respectively (Fig. 2D) (22). CHIP KD had a marginal effect on slow endocytosis of rΔF508CFTR in the absence of thermal unfolding and wt CFTR (Fig. 2D). CHIP KD also partially restored rΔF508CFTR endocytic recycling (Fig. 2E) and delayed the lysosomal delivery from early endosomes (pH ~6.2) without interfering with Lamp2/CD63 lysosomal targeting and TfR recycling (fig. S4, C to E). In support of the CHIP involvement, ablating UbcH5c, a cognate E2 enzyme of CHIP, impeded the rΔF508CFTR removal from PM in IB3 and HeLa cells (Fig. 2, B and F). CHIP KD also reduced ubiquitination of complex-glycosylated rΔF508CFTR at 37°C to that at 26°C (Fig. 3, A and B), accounting for the attenuated internalization, facilitated recycling, and impeded lysosomal delivery of the unfolded CFTR.

Hsc70 recognizes unfolded CFTR at PM

In support of the CHIP loss-of-function phenotype, overexpression of CHIP wt but not the catalytically inactive CHIP-H260Q [in which His^{260} is replaced by Gln (25)] reduced rΔF508CFTR expression and metabolic stability by accelerating endocytosis in cotransfected COS7 cells (Fig. 3C and fig. S4F). Coimmunoprecipitation (co-IP) confirmed CHIP association with the core-glycosylated form (12) and revealed that CHIP physically interacted with complex-glycosylated rΔF508CFTR at 37°C (Fig. 3D). Weaker CHIP

binding, attributable to a milder structural defect of complex-glycosylated rΔF508CFTR compared with core-glycosylated F508CFTR (Fig. 1C), was stabilized by the CHIP-H260Q mutation, presumably by delaying CFTR dissociation (Fig. 3D). Abolishing Hsc70 and heat shock protein 90 (Hsp90) binding to the CHIP tetratricopeptide repeat (TPR) domain by a K30A mutation (replacement of Lys^{30} with Ala) (26) prevented channel down-regulation from PM (Fig. 3C and fig. S4F) and CHIP-rΔF508CFTR interaction (Fig. 3D). In accord with the Hsc70- and Hsp90-dependent CHIP interaction, association of Hsc70 and, to a lesser extent, Hsp90 with complex-glycosylated rΔF508CFTR, but less with its wt counterpart, was verified by co-IP (Fig. 3E).

Contribution of the molecular chaperones to the rΔF508CFTR peripheral QC was assessed in HeLa cells. Ablation of Hsc70 or Hsp90A (Hsp90α) stabilized rΔF508CFTR at PM (Fig. 3F and fig. S5A) by decreasing its ubiquitination (Fig. 3A, B, and G), internalization, lysosomal delivery, and degradation without interfering with TfR and CD4Tl-ccUb(AllRΔG) endocytosis and Lamp2/CD63 lysosomal sorting (Fig. 4, A to E), which phenocopied of the CHIP KD effect. Up-regulation of Hsp70 and a subset of cochaperones as part of the stress response induced by Hsc70 KD (fig. S6, C and F) was unable to compensate for the Hsc70 loss of function, which may imply functional differences among chaperones and cochaperones (27). CHIP-Hsc70 was previously shown to participate in the proteasomal and lysosomal degradation of PM-localized ErbB2 receptor, after the inhibition of Hsp90 by geldanamycin (28). It was noteworthy that geldanamycin had a minimal effect on the rΔF508CFTR PM stability (fig. S7), which highlighted the distinct initiating mechanism between rΔF508CFTR and ErbB2 degradation.

The role of CHIP-Hsc70 in the rΔF508CFTR ubiquitination was confirmed in vitro. Complex-glycosylated rΔF508CFTR-His_{10} was isolated by affinity chromatography under native conditions from BHK cells. Catalytic activity of recombinant wt and K30A, but not ΔUbox CHIP, was verified (fig. S8, A to D). Ubiquitination of rΔF508CFTR was reconstituted in the presence of E1, UbcH5c, CHIP, myc-Ub, and adenosine triphosphate (ATP) (Fig. 5A). Omitting any components or using CHIP-ΔUbox compromised the channel ubiquitination (Fig. 5A and fig. S8E). Similar results were obtained by using purified rΔF508CFTR from PM-enriched vesicles (Fig. 5B and fig. S8, F and G). Recombinant Hsc70 profoundly enhanced the CHIP-dependent ubiquitination, whereas CHIP-K30A remained ineffective (Fig. 5B and fig. S8E). Thus, Hsc70 plays an essential role in the recognition of nonnative rΔF508CFTR and CHIP recruitment in post-Golgi compartments. Wt CFTR was largely resistant to ubiquitination, which confirmed the conformational selectivity of the Hsc70-CHIP-UbcH5 complex in vitro (Fig. 5C) (12, 29).

Cochaperones regulate CFTR peripheral QC

The folding and degradative function of Hsc70-Hsp90 is regulated by cochaperones (24, 30–32). Functional screens using SMARTpool and single siRNAs revealed that BAG1, DNAJB2 (HSJ1), DNAJA1 (Hdj2), DNAJC7 (TPR2), HOP (STIP1), and Aha1 (AHSA1) were required for the rΔF508CFTR removal from PM of HeLa cells (Fig. 3F and fig. S5A). Hsc70 and its co-chaperones, BAG1, DNAJB2, DNAJA1, and HOP were also effective in IB3 cells, although Hsp90A and Aha1 had marginal impact (fig. S5B).

We verified the contribution of cochaperones to rΔF508CFTR disposal via ubiquitination, internalization, and lysosomal targeting. Ablation of the Hsc70 regulator DNAJA1, the Hsc70-Hsp90 coupling factor HOP, or the Hsp90 cochaperone Aha1 reduced the rΔF508CFTR ubiquitination (Fig. 3, B and G) and internalization without affecting TfR and CD4Tcc-Ub(AllRΔG) uptake (Fig. 4A and table S1). Correlation between the channel ubiquitination and internalization or PM stability suggests that these cochaperones facilitate rΔF508CFTR internalization and disposal by enhancing ubiquitination, presumably through regulation of the CHIP-Hsc70-Hsp90A complexes (fig. S5, C and D).

Lysosomal delivery of rΔF508CFTR from early endosomes was impeded by KD of DNAJA1, DNAJB2, DNAJC7, Aha1, BAG1, or HOP (Fig. 4B and fig. S9). Ablation of DNAJC7, Aha1, or HOP, however, also delayed the Lamp2/CD63 lysosomal targeting (Fig. 4C), which implied their Ub-independent function on cargo lysosomal targeting (table S1). In contrast, DNAJB2 was involved in the lysosomal targeting of rΔF508CFTR by enhancing ubiquitination only at early endosomes (Figs. 3, B and G, and 4, A to C). BAG1 KD selectively inhibited rΔF508CFTR internalization and lysosomal delivery without influencing ubiquitination (Figs. 3, B and G, and 4, A to C), which indicated that it functions after ubiquitination. Because BAG1 is ubiquitinated by CHIP and contains an Ub-like domain (30), it may link the chaperone-rΔF508CFTR complex to Ub-binding adaptors of the internalization and lysosomal-sorting machinery.

CFTR PM level is defined by its PM stability and biosynthetic secretion dictated by transcription, translation, and ER-associated folding and degradation rates. Based on the minimal effect of chaperone and cochaperone KD on the core-glycosylated ΔF508CFTR expression (fig. S5F) and ERAD (Fig. 4, D and E, see below), we inferred that CFTR PM density is primarily modulated by folding and/or secretion and PM stability. Thus, at constant secretion, the PM density should be proportional to CFTR peripheral stability. Indeed, ablation of Hsc70, DNAJB2, or Aha1 proportionally increased the rΔF508CFTR PM density and function (Fig. 5D, and figs. S5E and S10), which suggested that these chaperones or cochaperones are primarily involved in peripheral degradation. In contrast, ablation of CHIP or Hsp90A only slightly increased the channel PM density, whereas DNAJA1, BAG1, or HOP KD did not (Fig. 5D and fig. S5E), which suggested that peripheral stabilization was offset by impaired biosynthetic secretion. The observed relation between the PM density and stability also supports the established role of chaperones and cochaperones in CFTR folding [e.g. calnexin (CNX) (6, 33); BAG2 (30); p23; FKBP8 (24) and stability [calreticulin (CALR) (34)].

Discussion

Our results revealed a partial overlap between constituents of the CFTR QC at ER (4, 12, 16, 35, 36) and PM, which suggested that similar principles may govern the recognition of structurally defective channels at different cellular locations. This is in line with the capacity of CHIP-UbcH5c to synthesize Ub-chains with all possible linkages (37), conferring a recognition signal for channel degradation by proteasome (38) and Ub-binding endocytic and ESCRT adaptors in post-Golgi compartments (9). Comparison of ERAD and lysosomal degradation showed that only Hsc70 or BAG1 KD delayed the ΔF508CFTR ERAD, whereas

KD of any chaperone or cochaperone identified in our functional screens attenuated rΔF508CFTR degradation (Fig. 4, D and E), which implied that parallel QC pathways, including chaperone-independent systems (13, 14, 39), have evolved to enhance the fidelity of the ER QC.

Based on our results and proteostatic mechanisms at different subcellular locations (1–4, 30), the following model is proposed for the peripheral CFTR QC (Fig. 5E). Recognition of unfolded cytoplasmic regions of CFTR is mediated by Hsc70 in concert with DNAJA1 and possibly by the Hsp90 machinery. Prolonged interaction with the chaperone–cochaperone complex recruits CHIP-UbcH5c and leads to ubiquitination of conformationally damaged CFTR. This ubiquitination is probably influenced by other E3 ligases and deubiquitinating enzyme activities (40), culminating in accelerated endocytosis and lysosomal delivery mediated by Ub-binding clathrin adaptors and the ESCRT machinery, respectively. Promiscuous substrate specificity of Hsc70-Hsp90 toward nonnative polypeptides implies that the peripheral QC probably contributes to triage decision of other conformationally defective PM proteins and thereby to pathogenesis of a variety of conformational diseases.

Supplementary Material

Refer to Web version on PubMed Central for supplementary material.

Acknowledgments

We thank J. Tavares and C. M. Mulvihill for CHIP purification and generating CFTR-His$_{10}$ cells, respectively; H. Stenmark for Hrs antibody; and H. Lewis, C. Lima, and K. Iwai for NBD1-3S, SUMO, Ulp1, and UbcH5 plasmids, respectively. Lamp1, Lamp2, and CD63 antibodies were developed by J. August and J. Hildreth (University of Iowa). T.O. and W.M.R. were supported by a Canadian Cystic Fibrosis Foundation and a Groupe de Recherche Axé sur la Structure des Protéines (GRASP) postdoctoral fellowship, respectively. This work was supported by grants to J.H. from Deutsche Forschungsgemeinschaft, J.C.Y. and G.L.L. from the Canadian Institute of Health Resources, NIH, Cystic Fibrosis Foundation Therapeutics, the Canadian Cystic Fibrosis Foundation, and the Canadian Foundation for Innovation. J.C.Y. and G.L.L. are holders of Canada Research Chairs.

References and Notes

1. Anelli T, Sitia R. EMBO J. 2008; 27:315. [PubMed: 18216874]
2. Hebert DN, Molinari M. Physiol Rev. 2007; 87:1377. [PubMed: 17928587]
3. Powers ET, Morimoto RI, Dillin A, Kelly JW, Balch WE. Annu Rev Biochem. 2009; 78:959. [PubMed: 19298183]
4. Vembar SS, Brodsky JL. Nat Rev Mol Cell Biol. 2008; 9:944. [PubMed: 19002207]
5. Sharma M, et al. J Cell Biol. 2004; 164:923. [PubMed: 15007060]
6. Glozman R, et al. J Cell Biol. 2009; 184:847. [PubMed: 19307599]
7. Hayashi H, Sugiyama Y. Mol Pharmacol. 2009; 75:143. [PubMed: 18829893]
8. Dupré S, Urban-Grimal D, Haguenauer-Tsapis R. Biochim Biophys Acta. 2004; 1695:89. [PubMed: 15571811]
9. Hurley JH, Emr SD. Annu Rev Biophys Biomol Struct. 2006; 35:277. [PubMed: 16689637]
10. Arvan P, Zhao X, Ramos-Castaneda J, Chang A. Traffic. 2002; 3:771. [PubMed: 12383343]
11. Alberti S, Böhse K, Arndt V, Schmitz A, Höhfeld J. Mol Biol Cell. 2004; 15:4003. [PubMed: 15215316]
12. Meacham GC, Patterson C, Zhang W, Younger JM, Cyr DM. Nat Cell Biol. 2001; 3:100. [PubMed: 11146634]
13. Younger JM, et al. Cell. 2006; 126:571. [PubMed: 16901789]

14. Morito D, et al. Mol Biol Cell. 2008; 19:1328. [PubMed: 18216283]
15. Denning GM, et al. Nature. 1992; 358:761. [PubMed: 1380673]
16. Younger JM, et al. J Cell Biol. 2004; 167:1075. [PubMed: 15611333]
17. Grove DE, Rosser MF, Ren HY, Naren AP, Cyr DM. Mol Biol Cell. 2009; 20:4059. [PubMed: 19625452]
18. Pedemonte N, et al. J Clin Invest. 2005; 115:2564. [PubMed: 16127463]
19. Materials and methods are available as supporting material on *Science* Online.
20. Du K, Sharma M, Lukacs GL. Nat Struct Mol Biol. 2005; 12:17. [PubMed: 15619635]
21. Sharma M, Benharouga M, Hu W, Lukacs GL. J Biol Chem. 2001; 276:8942. [PubMed: 11124952]
22. Barriere H, et al. Traffic. 2006; 7:282. [PubMed: 16497223]
23. Staub O, Rotin D. Physiol Rev. 2006; 86:669. [PubMed: 16601271]
24. Wang X, et al. Cell. 2006; 127:803. [PubMed: 17110338]
25. Single-letter abbreviations for the amino acid residues used in this article are as follows: A, Ala; H, His; K, Lys; and Q, Gln.
26. Ballinger CA, et al. Mol Cell Biol. 1999; 19:4535. [PubMed: 10330192]
27. Goldfarb SB, et al. Proc Natl Acad Sci USA. 2006; 103:5817. [PubMed: 16585520]
28. Xu W, et al. Proc Natl Acad Sci USA. 2002; 99:12847. [PubMed: 12239347]
29. Murata S, Minami Y, Minami M, Chiba T, Tanaka K. EMBO Rep. 2001; 2:1133. [PubMed: 11743028]
30. Arndt V, Rogon C, Höhfeld J. Cell Mol Life Sci. 2007; 64:2525. [PubMed: 17565442]
31. Minami Y, Höhfeld J, Ohtsuka K, Hartl FU. J Biol Chem. 1996; 271:19617. [PubMed: 8702658]
32. Tzankov S, Wong MJ, Shi K, Nassif C, Young JC. J Biol Chem. 2008; 283:27100. [PubMed: 18684711]
33. Okiyoneda T, et al. Mol Biol Cell. 2004; 15:563. [PubMed: 14595111]
34. Harada K, et al. J Biol Chem. 2006; 281:12841. [PubMed: 16527813]
35. Loo MA, et al. EMBO J. 1998; 17:6879. [PubMed: 9843494]
36. Meacham GC, et al. EMBO J. 1999; 18:1492. [PubMed: 10075921]
37. Zhang M, et al. Mol Cell. 2005; 20:525. [PubMed: 16307917]
38. Finley D. Annu Rev Biochem. 2009; 78:477. [PubMed: 19489727]
39. Sato BK, Schulz D, Do PH, Hampton RY. Mol Cell. 2009; 34:212. [PubMed: 19394298]
40. Bomberger JM, Barnaby RL, Stanton BA. J Biol Chem. 2009; 284:18778. [PubMed: 19398555]

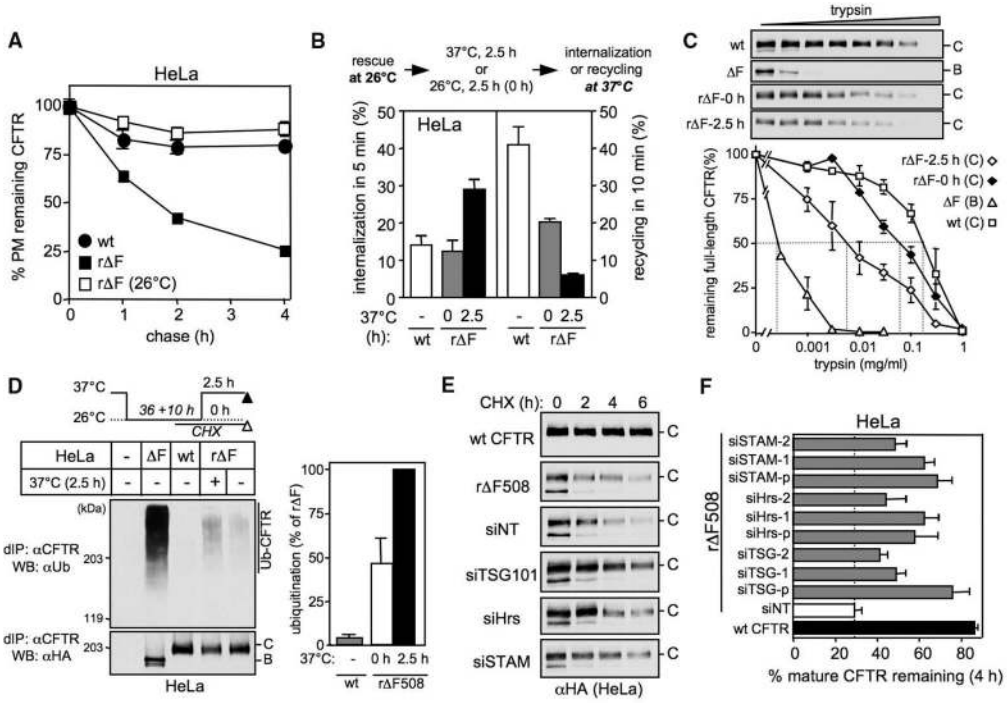

Fig. 1.

Conformationally destabilized rΔF508CFTR is ubiquitinated and targeted for ESCRT-dependent degradation. (**A**) CFTR PM stability was determined by enzyme-linked immunosorbent assay (ELISA). ΔF508CFTR was rescued at 26°C for 36 hours, followed by 37°C incubation for 2.5 hours (rΔF) or at 26°C. (**B**) (Left) CFTR internalization and (right) endocytic recycling were measured by ELISA. Unfolding of rΔF508CFTR was accomplished at 37°C (2.5 hours). (**C**) Trypsin susceptibility of CFTR variants in microsomes was measured by quantifying the remaining full-length CFTR with immunoblotting and densitometry. Bands B and C indicate core- and complex-glycosylated CFTR, respectively. (**D**) rΔF508CFTR ubiquitination in post-Golgi compartments was measured by d-IP and normalized for CFTR in precipitates. Nonrescued ΔF508CFTR (ΔF) was used as a positive control. (**E** and **F**) Metabolic stability of rΔF508CFTR was measured by CHX chase at 37°C and immunoblotting with an antibody against HA in ESCRT KD HeLa cells (E). Remaining complex-glycosylated CFTR was quantified by densitometry and expressed as a percentage of the initial amount (F). SMARTpool (p) or single siRNA (1 and 2) were used. siNT; nontargeted siRNA.

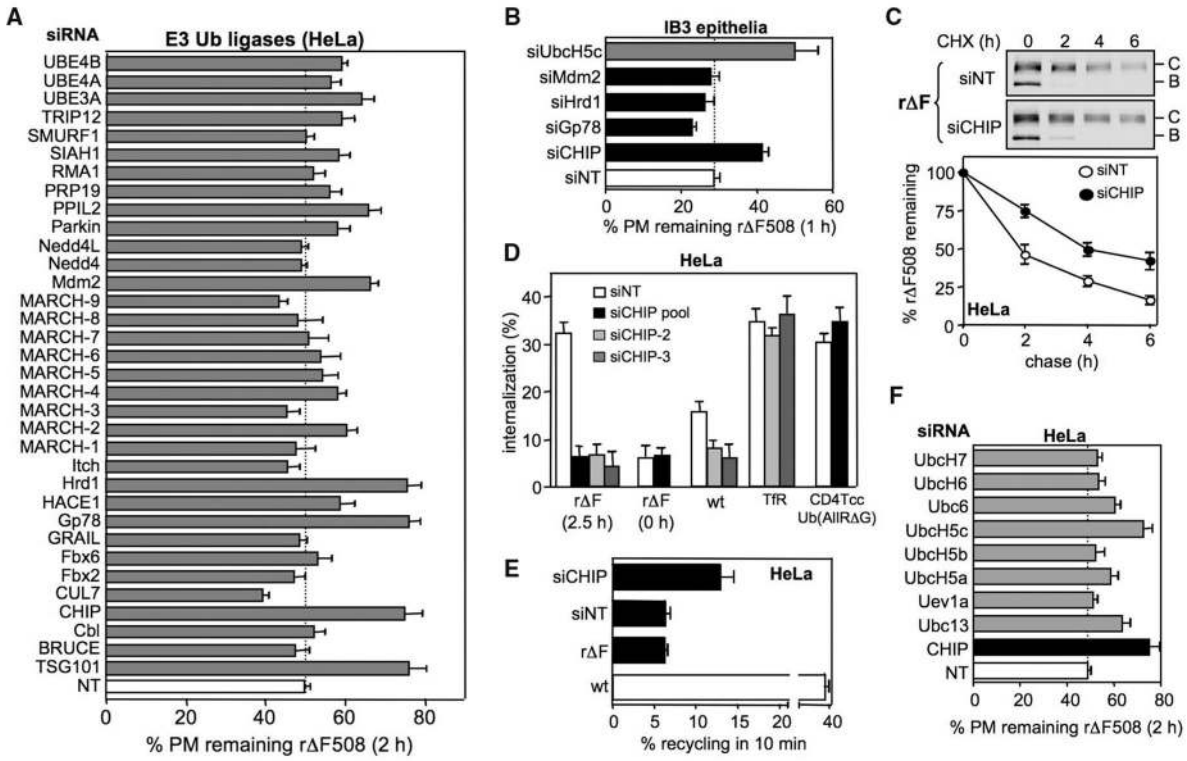

Fig. 2.

CHIP mediates rΔF508CFTR elimination from PM. (**A**) Functional siRNA screen to identify Ub ligases responsible for rΔF508CFTR elimination from PM in HeLa cells. Ub ligases were knocked down by 50 nM SMARTpool siRNA, and rΔF508CFTR PM stability was measured at 37°C by ELISA. TSG101 siRNA; positive control. Data are means ± SEM from two or three independent quadruplicate experiments. (**B**) Effect of Ub ligase or UbcH5c KD on rΔF508CFTR PM stability in IB3 cells. (**C**) rΔF508CFTR metabolic stability in post-Golgi compartments was measured by immunoblotting with CHX chase upon CHIP KD by SMARTpool siRNA. Remaining complex-glycosylated CFTR was plotted. (**D**) Internalization of CFTRs (5 min), TfR (5 min), and CD4Tcc-Ub(AllRΔG) (2.5 min) were measured at 37°C in CHIP-KD cells. (**E**) CHIP KD enhanced rΔF508CFTR endocytic recycling. (**F**) rΔF508CFTR PM stability in E2-KD cells was measured as in (A).

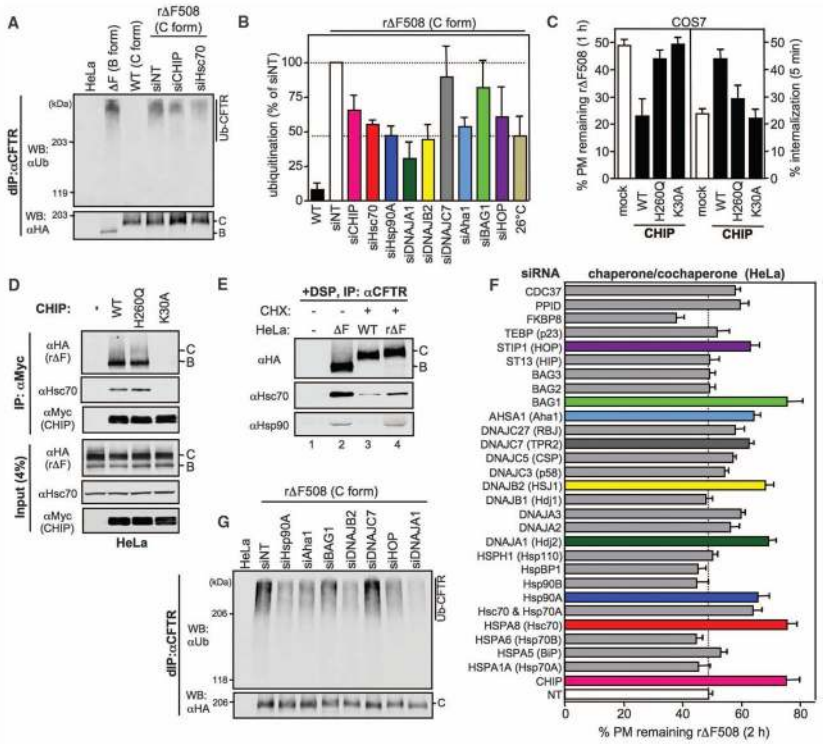

Fig. 3.

rΔF508CFTR ubiquitination is regulated by chaperones and co-chaperones. (**A**) rΔF508CFTR ubiquitination in post-Golgi compartments was measured in SMARTpool siRNA-transfected HeLa cells as in Fig. 1D. (**B**) Quantification of CFTR ubiquitination in immunoblots (A) and (G). Signal was normalized for CFTR in precipitates and expressed as percentages of rΔF508CFTR ubiquitination in siNT-treated cells after unfolding (37°C, 2.5 hours) as in Fig. 1D. (**C**) (Left) PM stability and (right) internalization of rΔF508CFTR were measured by ELISA in COS7 cells coexpressing myc-CHIP variants. (**D**) CHIP interacts with core- and complex-glycosylated rΔF508CFTR in HeLa cells transfected with myc-CHIP variants. (**E**) Interaction of chaperones with complex-glycosylated rΔF508CFTR was shown by co-IP in HeLa cells after in vivo cross-linking by 0.1 mM dithiobis[succinimidyl propionate] (DSP). Core-glycosylated wt and rΔF508CFTR were minimized by CHX chase (lanes 3 and 4). (**F**) rΔF508CFTR PM stability was evaluated upon KD of chaperone or cochaperone by SMARTpool siRNA as in Fig. 2A. Data are means ± SEM from two or three independent quadruplicate experiments. (**G**) rΔF508CFTR ubiquitination in post-Golgi compartments was measured in SMARTpool siRNA-transfected HeLa cells as in (A).

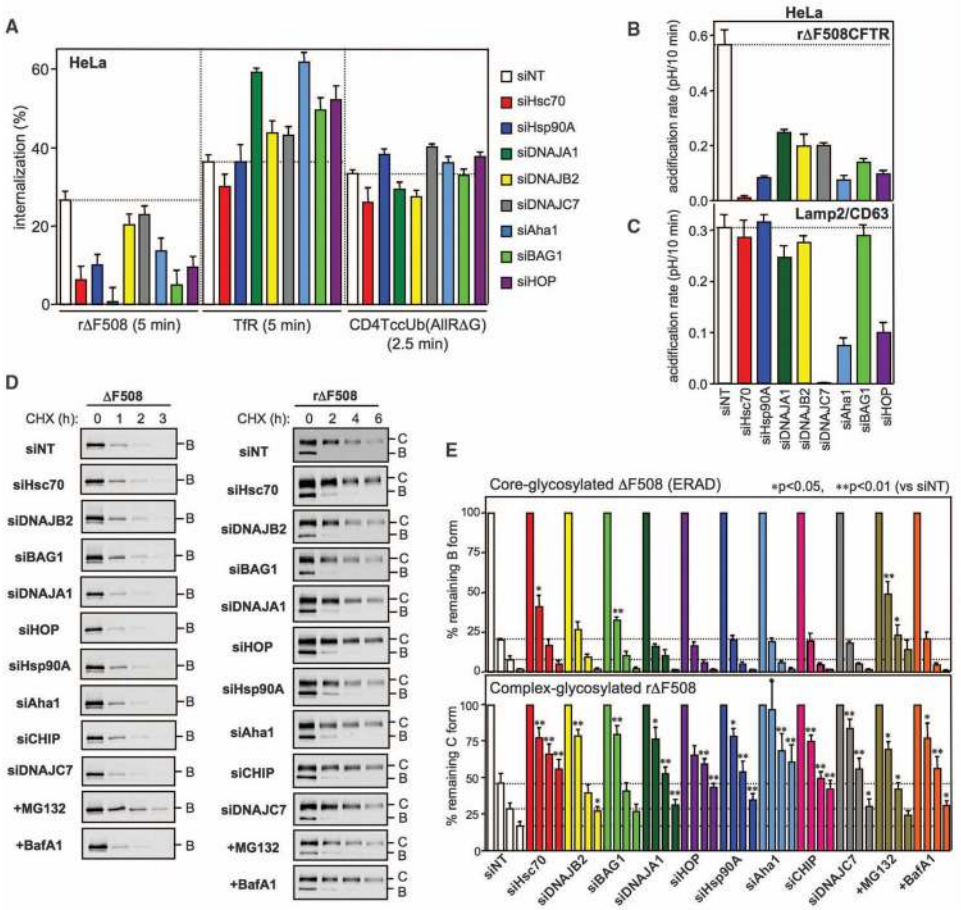

Fig. 4.

Internalization and lysosomal targeting of rΔF508CFTR are regulated by distinct sets of chaperones and cochaperones. (**A**) Internalization of unfolded rΔF508CFTR (5 min), TfR (5 min) and CD4Tcc-Ub(AllRΔG) (2.5 min) was determined as in Fig. 2D. (**B** and **C**) Effect of chaperone or cochaperone KD on lysosomal sorting of (B) rΔF508CFTR and (C) Lamp2/CD63 was examined by measuring the acidification rate from early endosomes to lysosomes (see fig. S9). (**D**) Metabolic stability of (left) core-glycosylated ΔF508CFTR and (right) complex-glycosylated rΔF508CFTR in SMARTpool siRNA-transfected HeLa cells was determined by immunoblotting with CHX chase. (**E**) CFTR disappearance was quantified by densitometry and expressed as percentages of initial amount (T-0) in experiments shown in (D). Bar graphs of each sample represent the data (top) at 0- to 3-hour and (bottom) 0- to 6-hour chase. MG132 and bafilomycin A1 (BafA1) were positive controls for ERAD and lysosomal degradation, respectively.

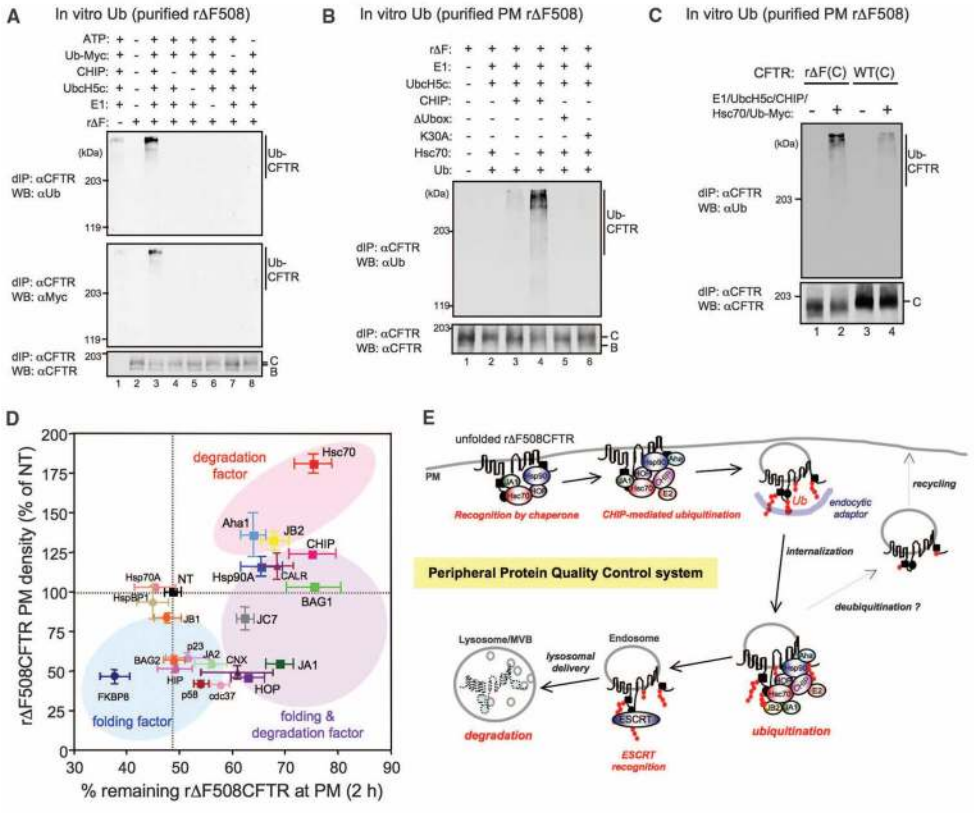

Fig. 5.

The peripheral QC machinery ubiquitinates the unfolded CFTR and dictates the PM level. (**A**) Reconstitution of rΔF508CFTR ubiquitination in vitro. Purified complex-glycosylated rΔF508CFTR-His_{10} was incubated with E1, UbcH5c, CHIP, Hsc70, Ub-Myc, and ATP at 30°C for 2 hours. rΔF508CFTR was isolated by d-IP and analyzed by immunoblotting. (**B**) CHIP-dependent ubiquitination of purified rΔF508CFTR from PM-enriched vesicles was stimulated by recombinant Hsc70. (**C**) Wt and rΔF508 CFTR-His_{10} were purified and ubiquitinated as in (B). (**D**) Classification of chaperones/cochaperones based on their effect on rΔF508CFTR PM density (fig. S5E) and stability (Figs. 2A and 3F). Components of the peripheral QC machinery identified are indicated by larger type. (**E**) Working model for the peripheral protein QC of rΔF508CFTR.